



ELSEVIER

Contents lists available at ScienceDirect

## Journal of Computational Physics

www.elsevier.com/locate/jcp



## Semi-implicit spectral deferred correction methods for highly nonlinear partial differential equations

Ruihan Guo <sup>a,1</sup>, Yinhua Xia <sup>b,2</sup>, Yan Xu <sup>b,\*,3</sup><sup>a</sup> School of Mathematics and Statistics, Zhengzhou University, Zhengzhou, Henan 450001, PR China<sup>b</sup> School of Mathematical Sciences, University of Science and Technology of China, Hefei, Anhui 230026, PR China

## ARTICLE INFO

## Article history:

Received 17 October 2016

Received in revised form 21 February 2017

Accepted 23 February 2017

Available online 2 March 2017

## Keywords:

Semi-implicit spectral deferred correction method

Highly nonlinear partial differential equations

Local discontinuous Galerkin method

High order accuracy

## ABSTRACT

The goal of this paper is to develop a novel semi-implicit spectral deferred correction (SDC) time marching method. The method can be used in a large class of problems, especially for highly nonlinear ordinary differential equations (ODEs) without easily separating of stiff and non-stiff components, which is more general and efficient comparing with traditional semi-implicit SDC methods. The proposed semi-implicit SDC method is based on low order time integration methods and corrected iteratively. The order of accuracy is increased for each additional iteration. And we also explore its local truncation error analytically. This SDC method is intended to be combined with the method of lines, which provides a flexible framework to develop high order semi-implicit time marching methods for nonlinear partial differential equations (PDEs). In this paper we mainly focus on the applications of the nonlinear PDEs with higher order spatial derivatives, e.g. convection diffusion equation, the surface diffusion and Willmore flow of graphs, the Cahn–Hilliard equation, the Cahn–Hilliard–Brinkman system and the phase field crystal equation. Coupled with the local discontinuous Galerkin (LDG) spatial discretization, the fully discrete schemes are all high order accurate in both space and time, and stable numerically with the time step proportional to the spatial mesh size. Numerical experiments are carried out to illustrate the accuracy and capability of the proposed semi-implicit SDC method.

© 2017 Elsevier Inc. All rights reserved.

## 1. Introduction

In this paper, we will develop a novel semi-implicit spectral deferred correction (SDC) time marching method for solving time dependent highly nonlinear partial differential equations (PDEs) containing high order spatial derivatives. Coupling with the local discontinuous Galerkin (LDG) spatial discretization, we develop an arbitrary high order accurate and stable schemes for convection diffusion equation, the surface diffusion and Willmore flow of graphs, the Cahn–Hilliard equation, the Cahn–Hilliard–Brinkman system and the phase field crystal equation. Due to the local property of the LDG methods, the resulting implicit scheme is easy to implement and can be solved in an explicit way when it is coupled with iterative methods.

\* Corresponding author.

E-mail addresses: [rguo@zzu.edu.cn](mailto:rguo@zzu.edu.cn) (R. Guo), [yhxia@ustc.edu.cn](mailto:yhxia@ustc.edu.cn) (Y. Xia), [yxu@ustc.edu.cn](mailto:yxu@ustc.edu.cn) (Y. Xu).<sup>1</sup> Research supported by NSFC grant No. 11601490.<sup>2</sup> Research supported by NSFC grant Nos. 11471306, 11371342.<sup>3</sup> Research supported by NSFC grant Nos. 11371342, 11626253, 91630207.

The discontinuous Galerkin (DG) method is a class of finite element methods, in which using a completely discontinuous piecewise polynomials as the numerical solution and the test spaces. It was first designed as a method for solving hyperbolic conservation laws containing only first order spatial derivatives, e.g. Reed and Hill [26] for solving linear equations, and Cockburn et al. [5–8] for solving nonlinear problems.

It is difficult to apply the DG method directly to PDEs containing higher order spatial derivatives, therefore the LDG method was introduced. The idea of the LDG method is to rewrite the equations with higher order derivatives as a first order system, then apply the DG method to the system. The first LDG method was constructed by Cockburn and Shu [9] for solving nonlinear convection diffusion equations containing second order spatial derivatives. Then LDG methods have been successfully designed and applied in a number of models involving diffusion and dispersive problems (see for example the review paper [33]). DG and LDG methods also have several attractive properties, for example: allowing for efficient  $h$ ,  $p$  adaptivity and having excellent parallel efficiency. The most important property of DG and LDG methods is high order accurate, which motivates us to develop high order temporal accuracy scheme to get the goal of obtaining high order accuracy in both space and time together with robust stability conditions.

By the method of lines, the application of the LDG method for spatial variables for a partial differential equation will generate a large coupled system of ordinary differential equations (ODEs). The development of suitable solvers for solving different types of ODEs have attracted a lot of attention in the last decades. For non-stiff ODEs, there exist extremely effective high order explicit methods [1,4,21], such as Runge–Kutta, linear multi-step and predictor corrector methods. For stiff problems, the situation is considerably more complicated, but still many efficient implicit methods [1,4,22] have been developed. Nevertheless, Dutt et al. constructed a new variation of the classical method of deferred corrections, the SDC method in [13], which preserve good stability and accuracy properties for stiff problems. Tang et al. provided a general framework for the convergence of the SDC method in [27].

In some cases, the resulting ODEs include both stiff term  $F_S$  and non-stiff term  $F_N$ , and can be written as

$$\begin{cases} u_t = F_S(t, u(t)) + F_N(t, u(t)), & t \in [0, T] \\ u(0) = u_0. \end{cases} \quad (1.1)$$

An efficient time marching technique to solve the ODEs (1.1) is semi-implicit methods, which treats the stiff component  $F_S$  implicitly and the non-stiff component  $F_N$  explicitly. For example, Minion developed an efficient semi-implicit SDC method for solving the ODEs (1.1). Xia, Xu and Shu [29] explored the SDC method, the additive Runge–Kutta (ARK) method and the exponential time differencing (ETD) method for the LDG methods to solve PDEs with higher order spatial derivatives, which were all validated to be effective. The existing semi-implicit SDC methods have been developed to solve many problems, such as the phase field problems [15,24,31] and the phase field crystal equation [19]. Unfortunately, these semi-implicit time marching methods are mainly efficient for problems with easily separate stiff and non-stiff components.

However, it is not always easy to separate the stiff and non-stiff components, and therefore the use of traditional semi-implicit schemes is not straightforward. In such cases, one usually relies on fully implicit schemes. But, fully implicit schemes have the disadvantages of difficult implementation and poor stability properties. To get a suitable solver for this class of problems, Boscarino et al. [2] developed several semi-implicit Runge–Kutta schemes up to order three for time-dependent highly nonlinear PDEs. Guo, Filbet and Xu [20] applied the semi-implicit Runge–Kutta methods coupled with LDG spatial discretization to solve a series of highly nonlinear PDEs containing higher order spatial derivatives, obtaining second order and third order accuracy in both time and space. Motivated by this idea and the desire to develop higher order temporal accuracy, we will propose a novel semi-implicit SDC method for highly nonlinear PDEs, namely, the stiff and non-stiff components can not be well separated. The semi-implicit Runge–Kutta method introduced in [20] and the SDC method proposed here are all efficient for highly nonlinear PDEs. However, the Runge–Kutta method has some limitations, for example, it is more difficult to construct for higher order accuracy. While for the SDC method, an advantage of this method is that it is a one step method and can be constructed easily and systematically for any order of accuracy.

In this paper, we will apply the proposed semi-implicit SDC method to solve a series of highly nonlinear time dependent PDEs, namely, the nonlinear convection diffusion equation, the surface diffusion and Willmore flow of graphs, the Cahn–Hilliard equation with degenerate mobility, the Cahn–Hilliard–Brinkman system and the phase field crystal equation. Convex splitting schemes were developed by Guo and Xu for the Cahn–Hilliard equation [17], the Cahn–Hilliard–Brinkman system [18] and the phase field crystal equation [19], which were unconditionally energy stable. However, these schemes are only first order or second order accurate in time. Based on the first order schemes, the proposed semi-implicit SDC method can therefore be applied to improve the temporal accuracy. The surface diffusion and Willmore flow of graphs are both highly nonlinear fourth-order PDEs, high order semi-implicit time marching methods are difficult to construct and therefore are desirable to develop.

The organization of the paper is as follows. In Section 2, we develop a novel high order semi-implicit SDC method for a general class of ODEs and study its local truncation error analytically. Numerical experiments are carried out in Section 3, testing the performance of the semi-implicit SDC method coupled with the LDG spatial discretization for solving a series of highly nonlinear PDEs, including the nonlinear convection diffusion equation, the surface diffusion and Willmore flow of graphs, the Cahn–Hilliard equation with degenerate mobility, the Cahn–Hilliard–Brinkman system and the phase field crystal equation. Finally, we give concluding remarks in Section 4.

## 2. The semi-implicit SDC methods

The SDC method was first constructed by Dutt, Greengard and Rokhlin [13] to develop high order stable methods for stiff and non-stiff problems. Then, a semi-implicit SDC method was introduced in [25] to solve ODEs containing both stiff and non-stiff components. The method is very efficient for PDEs with easily separate stiff and non-stiff components, which treats the stiff terms implicitly and the non-stiff terms explicitly. The classical semi-implicit SDC method proposed in [25] will first be reviewed in Subsection 2.1.

However, it is not always easy to separate the stiff and non-stiff components, especially for highly nonlinear ODEs. In Subsection 2.2, we will propose a novel semi-implicit SDC method to solve this kind of ODEs. It is no doubt that the proposed SDC method is a useful extension of the classical semi-implicit SDC method.

### 2.1. The classical semi-implicit SDC method

The basic idea of the SDC method is to replace the original ODEs by the corresponding Picard integral equation and discretize it on a sequence of large time intervals by using a Legendre–Gauss type quadrature. The resulting system is first solved by a simple time marching method, and then are corrected iteratively, with the order of accuracy increased by one for each additional iteration.

Supposing now one ODE can be written as

$$\begin{cases} u_t = F_S(t, u(t)) + F_N(t, u(t)), & t \in [0, T] \\ u(0) = u_0, \end{cases} \quad (2.1)$$

where  $F_S$  is a stiff term and  $F_N$  is a non-stiff term. The details of the semi-implicit SDC method proposed in [25] are described in the following.

Suppose now the time interval  $[0, T]$  is divided into  $M$  non-overlapping intervals by the partition  $0 = t_0 < t_1 < \dots < t_n < \dots < t_M = T$ . We shall describe below the semi-implicit SDC method which will be used to advance from  $t_n$  to  $t_{n+1}$ . Let  $\Delta t_n = t_{n+1} - t_n$  and  $u_n$  denotes the numerical approximation of  $u(t_n)$ , with  $u_0 = u(0)$ .

Divide the time interval  $[t_n, t_{n+1}]$  into  $P$  subintervals by choosing the points  $t_{n,m}$  for  $m = 0, 1, \dots, P$  such that  $t_n = t_{n,0} < t_{n,1} < \dots < t_{n,m} < \dots < t_{n,P} = t_{n+1}$ . Let  $\Delta t_{n,m} = t_{n,m+1} - t_{n,m}$  and  $u_{n,m}^k$  denotes the  $k$ th order approximation to  $u(t_{n,m})$ . The points  $\{t_{n,m}\}_{m=0}^P$  can be chosen to be the Chebyshev Gauss–Lobatto nodes on  $[t_n, t_{n+1}]$  to avoid the instability of approximation at equispaced nodes for high order accuracy. We can also choose the Gauss nodes, or Legendre Gauss–Radau nodes or Legendre Gauss–Lobatto nodes. Starting from  $u_n$ , we give the algorithm to calculate  $u_{n+1}$  in the following.

#### Compute the initial approximation:

$$u_{n,0}^1 = u_n.$$

Use a first order semi-implicit scheme to compute approximate solution  $u^1$  at the nodes  $\{t_{n,m}\}_{m=1}^P$ , i.e.

For  $m = 0, \dots, P - 1$

$$u_{n,m+1}^1 = u_{n,m}^1 + \Delta t_{n,m} (F_S(t_{n,m+1}, u_{n,m+1}^1) + F_N(t_{n,m}, u_{n,m}^1)). \quad (2.2)$$

#### Compute successive corrections based on first order scheme:

For  $k = 1, \dots, K$

$$u_{n,0}^{k+1} = u_n.$$

For  $m = 0, \dots, P - 1$

$$\begin{aligned} u_{n,m+1}^{k+1} = & u_{n,m}^{k+1} + \Delta t_{n,m} (F_S(t_{n,m+1}, u_{n,m+1}^{k+1}) - F_S(t_{n,m+1}, u_{n,m+1}^k)) \\ & + \Delta t_{n,m} (F_N(t_{n,m}, u_{n,m}^{k+1}) - F_N(t_{n,m}, u_{n,m}^k)) + I_m^{m+1} (F_S(t, u^k) + F_N(u^k)), \end{aligned} \quad (2.3)$$

where  $I_m^{m+1} (F_S(t, u^k) + F_N(u^k))$  is the integral of the  $P$ -th degree interpolating polynomial on the  $P + 1$  points  $(t_{n,m}, F_S(t_{n,m}, u_{n,m}^k) + F_N(t_{n,m}, u_{n,m}^k))_{m=0}^P$  over the subinterval  $[t_{n,m}, t_{n,m+1}]$ .

Finally we have  $u_{n+1} = u_{n,P}^{K+1}$ .

### 2.2. The novel semi-implicit SDC method

Minion mentioned in [25] that it is not always trivial to find such a splitting (2.1) for an ODE. For example, we consider here a more general class of problem of the form

$$\begin{cases} u_t = F(t, u(t), u(t)), & t \in [0, T], \\ u(0) = u_0, \end{cases} \quad (2.4)$$

where  $u_0, u(t) \in \mathbb{R}^n$  and  $F : \mathbb{R} \times \mathbb{R}^n \times \mathbb{R}^n \rightarrow \mathbb{R}^n$ . Requiring that  $F \in C^1(\mathbb{R} \times \mathbb{R}^n \times \mathbb{R}^n)$  is, of course, sufficient to guarantee local existence and uniqueness of the solution to (2.4). And the dependence on the second argument of  $F$  is non-stiff, while

the dependence on the third argument of  $F$  is stiff. In fact, all the cases mentioned before belong to this more general class, including the stiff, non-stiff problems and the problems containing separate stiff and non-stiff components.

In the above case, the classical semi-implicit SDC method described in Subsection 2.1 is not efficient anymore. Because if we treat the right term  $F(t, u(t), u(t))$  of (2.4) as a non-stiff term and apply the existing semi-implicit SDC method, we can get the initial approximation as follows

$$u_{n,m+1}^1 = u_{n,m}^1 + \Delta t_{n,m} F(t_{n,m}, u_{n,m}^1, u_{n,m}^1), \tag{2.5}$$

which in fact is a forward Euler method, and it has severe time step restriction to maintain the stability. While when we treat it as a stiff term, the initial approximation is in the following form

$$u_{n,m+1}^1 = u_{n,m}^1 + \Delta t_{n,m} F(t_{n,m+1}, u_{n,m+1}^1, u_{n,m+1}^1). \tag{2.6}$$

It is a fully implicit scheme, which will incredibly increase the difficulty of implementation.

Therefore, it will be desirable to develop a novel semi-implicit SDC method to solve the ODE (2.4). The main idea of the method is that the variable  $u(t)$  appearing as the second argument of  $F$  is treated explicitly, while  $u(t)$  appearing as the third argument is treated implicitly. We shall describe below the new semi-implicit SDC method which will be used to advance from  $t_n$  to  $t_{n+1}$ .

**Compute the initial approximation:**

$$u_{n,0}^1 = u_n.$$

Use a first order semi-implicit scheme to compute approximate solution  $u^1$  at the nodes  $\{t_{n,m}\}_{m=1}^P$ , i.e.

For  $m = 0, \dots, P - 1$

$$u_{n,m+1}^1 = u_{n,m}^1 + \Delta t_{n,m} F(t_{n,m}, u_{n,m}^1, u_{n,m+1}^1). \tag{2.7}$$

**Compute successive corrections based on first order scheme:**

For  $k = 1, \dots, K$

$$u_{n,0}^{k+1} = u_n.$$

For  $m = 0, \dots, P - 1$

$$u_{n,m+1}^{k+1} = u_{n,m}^{k+1} + \theta \Delta t_{n,m} (F(t_{n,m+1}, u_{n,m+1}^k, u_{n,m+1}^{k+1}) - F(t_{n,m+1}, u_{n,m+1}^k, u_{n,m+1}^k)) + I_m^{m+1}(F(t, u^k, u^k)), \tag{2.8}$$

where  $0 \leq \theta \leq 1$ ,  $I_m^{m+1}(F(t, u^k, u^k))$  is the integral of the  $P$ -th degree interpolating polynomial on the  $P + 1$  points  $(t_{n,m}, F(t_{n,m}, u_{n,m}^k, u_{n,m}^k))_{m=0}^P$  over the subinterval  $[t_{n,m}, t_{n,m+1}]$ , which is the numerical quadrature approximation of

$$\int_{t_{n,m}}^{t_{n,m+1}} F(\tau, u(\tau), u(\tau)) d\tau.$$

Finally we have  $u_{n+1} = u_{n,P}^{K+1}$ .

Here, we will specify how to compute  $I_m^{m+1}(F(t, u^k, u^k))$ . Firstly, we approximate  $F(t, u^k, u^k)$  by its Lagrange interpolation polynomials  $F_P(t, u^k, u^k)$  based on the Gauss type points, namely

$$F_P(t, u^k, u^k) = \sum_{j=0}^P F_P(t_{n,j}, u_{n,j}^k, u_{n,j}^k) \mathcal{L}_j^P(t). \tag{2.9}$$

Then, we approximate  $I_m^{m+1}(F(t, u^k, u^k))$  by

$$I_m^{m+1}(F(t, u^k, u^k)) \approx \int_{t_{n,m}}^{t_{n,m+1}} F_P(t, u^k, u^k) dt = \sum_{j=1}^P F_P(t_{n,j}, u_{n,j}^k, u_{n,j}^k) c_{m,j}^P, \tag{2.10}$$

where

$$c_{m,j}^P = \int_{t_{n,m}}^{t_{n,m+1}} \mathcal{L}_j^P(t) dt \tag{2.11}$$

can be precomputed once and for all.

2.3. The local truncation error

**Lemma 2.1.** (Local truncation error). The local truncation error obtained with the proposed semi-implicit SDC scheme is

$$\mathcal{O}(h^{\min[K+1, P+1]}), \tag{2.12}$$

where  $h = \max_{n,m} \Delta t_{n,m}$ .

**Proof.** Assume  $u_{n,0}^k = u(t_n)$ ,  $k = 1, \dots, K + 1$ . Taking the difference of

$$u(t_{n,m+1}) = u(t_{n,m}) + \int_{t_{n,m}}^{t_{n,m+1}} F(\tau, u(\tau), u(\tau))d\tau \tag{2.13}$$

and (2.8), we have

$$\begin{aligned} u(t_{n,m+1}) - u_{n,m+1}^{k+1} &= u(t_{n,m}) - u_{n,m}^{k+1} \\ &\quad - \theta \Delta t_{n,m} (F(t_{n,m+1}, u_{n,m+1}^k, u_{n,m+1}^{k+1}) - F(t_{n,m+1}, u_{n,m+1}^k, u_{n,m+1}^k)) \\ &\quad + \int_{t_{n,m}}^{t_{n,m+1}} F(\tau, u(\tau), u(\tau))d\tau - I_m^{m+1}(F(t, u^k, u^k)). \end{aligned} \tag{2.14}$$

Here, we employ the induction strategy, and by induction on both  $m$  and  $k$ , when  $k = 1, m = 0$ ,

$$\begin{aligned} u(t_{n,1}) - u_{n,1}^2 &= u(t_{n,0}) - u_{n,0}^2 - \theta \Delta t_{n,0} (F(t_{n,1}, u_{n,1}^1, u_{n,1}^2) - F(t_{n,1}, u_{n,1}^1, u_{n,1}^1)) \\ &\quad + \int_{t_{n,0}}^{t_{n,1}} F(\tau, u(\tau), u(\tau)) - I_0^1(F(t, u^1, u^1)). \end{aligned}$$

We have

$$\begin{aligned} F(t_{n,1}, u_{n,1}^1, u_{n,1}^2) - F(t_{n,1}, u_{n,1}^1, u_{n,1}^1) &= F'_3(t_{n,1}, u_{n,1}^1, \xi)(u_{n,1}^2 - u_{n,1}^1) \\ &= F'_3(t_{n,1}, u_{n,1}^1, \xi)(u_{n,1}^2 - u(t_{n,1}) + u(t_{n,1}) - u_{n,1}^1), \\ &= F'_3(t_{n,1}, u_{n,1}^1, \xi)(u_{n,1}^2 - u(t_{n,1}) + \mathcal{O}(h^2)), \end{aligned}$$

and

$$\begin{aligned} \int_{t_{n,0}}^{t_{n,1}} F(\tau, u(\tau), u(\tau)) - I_0^1(F(t, u^1, u^1)) &= \int_{t_{n,0}}^{t_{n,1}} F(\tau, u(\tau), u(\tau))d\tau - I_0^1(F(t, u, u)) \\ &\quad + I_0^1(F(t, u, u)) - I_0^1(F(t, u^1, u^1)) \\ &= \mathcal{O}(h^3) + \mathcal{O}(h^3) \end{aligned} \tag{2.15}$$

In equation (2.15), we have used the fact that  $I_m^{m+1}(F(t, u, u))$  is the integral of the  $P$ -th degree interpolating polynomial on the  $P + 1$  points  $(t_{n,m}, F(u(t_{n,m}), u(t_{n,m})))_{m=0}^P$  over the subinterval  $[t_{n,m}, t_{n,m+1}]$ , which is accurate to the order  $\mathcal{O}(h^{P+2})$ . Based on all the analysis above, we have

$$u(t_{n,1}) - u_{n,1}^2 = \mathcal{O}(h^3). \tag{2.16}$$

Then we assume, when  $k \leq P$ ,

$$u(t_{n,l}) - u_{n,l}^k = \mathcal{O}(h^{k+1}), \quad \forall l \text{ in level } k, \tag{2.17}$$

$$u(t_{n,l}) - u_{n,l}^{k+1} = \mathcal{O}(h^{k+2}), \quad \text{for } l \leq m \text{ in level } k + 1. \tag{2.18}$$

Then we have

$$u(t_{n,m}) - u_{n,m}^{k+1} = \mathcal{O}(h^{k+2}),$$

$$\begin{aligned}
& F(t_{n,m+1}, u_{n,m+1}^k, u_{n,m+1}^{k+1}) - F(t_{n,m+1}, u_{n,m+1}^k, u_{n,m+1}^k) \\
&= F'_3(t_{n,m+1}, u_{n,m+1}^k, \xi)(u_{n,m+1}^{k+1} - u_{n,m+1}^k) \\
&= F'_3(t_{n,m+1}, u_{n,m+1}^k, \xi)(u_{n,m+1}^{k+1} - u(t_{n,m+1}) + u(t_{n,m+1}) - u_{n,m+1}^k) \\
&= F'_3(t_{n,m+1}, u_{n,m+1}^k, \xi)(u_{n,m+1}^{k+1} - u(t_{n,m+1}) + \mathcal{O}(h^{k+1})) \\
& \int_{t_{n,m}}^{t_{n,m+1}} F(\tau, u(\tau), u(\tau))d\tau - I_m^{m+1}(F(t, u^k, u^k)) \\
&= \int_{t_{n,m}}^{t_{n,m+1}} F(\tau, u(\tau), u(\tau))d\tau - I_m^{m+1}(F(t, u, u)) + I_m^{m+1}(F(t, u, u)) - I_m^{m+1}(F(t, u^k, u^k)) \\
&= \mathcal{O}(h^{P+2}) + \mathcal{O}(h^{k+2}) \\
&= \mathcal{O}(h^{k+2}).
\end{aligned}$$

Based on all the analysis above, we have

$$u(t_{n,m+1}) - u_{n,m+1}^{k+1} = \mathcal{O}(h^{\min[k+2, P+2]}). \quad \square \quad (2.19)$$

**Remark 2.1.** From the proof the local truncation error, we find that the term  $\theta \Delta t_{n,m} (F(t_{n,m+1}, u_{n,m+1}^k, u_{n,m+1}^{k+1}) - F(t_{n,m+1}, u_{n,m+1}^k, u_{n,m+1}^k))$  in the semi-implicit SDC scheme (2.8) does not affect the accuracy, but affect the stability of the scheme (e.g.,  $\theta = 0, 1$  for explicit and implicit scheme respectively). While the term  $I_m^{m+1}(F(t, u^k, u^k))$  in scheme (2.8) is responsible for the accuracy increasing. Since the order of accuracy is bounded by  $P + 1$ , usually we take  $k = P$  for efficiency in the application.

**Remark 2.2.** (Comparison with the existing semi-implicit Runge–Kutta method). In [20], we developed a semi-implicit Runge–Kutta method for highly nonlinear PDEs, and numerical experiments showed that it was indeed efficient. Comparing with the SDC method, it is more difficult to construct higher order Runge–Kutta scheme. Actually, only second order and third order temporal accuracy was achieved in [20]. While for the SDC method, an advantage of this method is that it is a one step method and can be constructed easily and systematically for any order of accuracy. Numerical experiments in Section 3 will then be presented to verify that we can indeed obtain higher order accuracy.

In addition, as mentioned in [25], in the Runge–Kutta methods, the solution computed during a time step is given by a particular linear combination of the right hand side of the ODE evaluated at intermediate or stage values, some of which have truncation errors of lower order accuracy than the final value. The linear combination is chosen such that the lower order truncation errors in the stage values cancel, and hence the exact form of these truncation errors must be known. This makes the generation of Runge–Kutta method for more than two disparate time scales very difficult. For the SDC method, low order intermediate solutions do not contribute directly to the final value. This allows for a straightforward extension to problems with more time scales.

For a detailed description of the comparison with the existing semi-implicit Runge–Kutta method, we refer readers to [25].

### 3. Applications

In this section, we perform numerical experiments for a series of highly nonlinear PDEs, including the nonlinear convection diffusion equation, the surface diffusion and Willmore flow of graphs, the Cahn–Hilliard equation with degenerate mobility, the Cahn–Hilliard–Brinkman system and the phase field crystal equation. These examples are used to verify that our spatial and time discretization methods can achieve high order accuracy in both space and time for PDEs without easily separating stiff and non-stiff components. In addition, we perform numerical tests for different kinds of PDEs to show the robustness of our semi-implicit SDC method. It is believable that the semi-implicit SDC method can be successfully applied to solve many other PDEs beyond those presented in this paper. All the computations are performed in double precision and on uniform spatial meshes.

In order to apply the proposed semi-implicit SDC method to solve highly nonlinear PDEs, we shall first discretize the PDEs in space to obtain a system of ODEs of the form (2.4). In this paper, we will restrict ourselves to the local discontinuous Galerkin (LDG) method for spatial discretization, which is high order accurate. For a detailed description of the LDG method as well as its implementation and applications, we refer readers to the lecture notes [10] and the review paper [11]. The corresponding LDG methods for the PDEs mentioned above can be found in [9,32,30,18,19].

**Table 3.1**  
Nonlinear convection–diffusion equation: accuracy test at time  $T = 0.5$ ,  $\Delta t = 0.1\Delta x$ .

|                 | $N$ | $L^2$ error | Order | $L^\infty$ error | Order |
|-----------------|-----|-------------|-------|------------------|-------|
| $\mathcal{P}^1$ | 16  | 3.00E–02    | –     | 2.60E–02         | –     |
|                 | 32  | 7.56E–03    | 1.99  | 7.26E–03         | 1.84  |
|                 | 64  | 1.89E–03    | 2.00  | 1.88E–03         | 1.95  |
| $\mathcal{P}^2$ | 16  | 3.03E–03    | –     | 2.97E–03         | –     |
|                 | 32  | 3.79E–04    | 3.00  | 3.84E–04         | 2.95  |
|                 | 64  | 4.73E–05    | 3.00  | 4.89E–05         | 2.97  |
| $\mathcal{P}^3$ | 16  | 2.75E–04    | –     | 3.34E–04         | –     |
|                 | 32  | 1.74E–05    | 3.98  | 2.30E–05         | 3.86  |
|                 | 64  | 1.09E–06    | 3.99  | 1.48E–06         | 3.96  |

Here, when the piecewise  $\mathcal{P}^1$  and  $\mathcal{P}^2$  elements are used in the LDG method, the third order semi-implicit SDC<sub>2</sub><sup>2</sup> method is used in the time integration. When the piecewise  $\mathcal{P}^3$  elements are used in the LDG method, we use the fourth order semi-implicit SDC<sub>3</sub><sup>3</sup> method.

In order to enhance the efficiency of the proposed approaches, the linear and nonlinear multigrid solvers [3] are used to solve the algebraic equations at each time step. For a detailed description of the multigrid solvers coupled with LDG spatial discretization and semi-implicit time marching method to solve PDEs, we refer readers to [17]. Due to the local properties of the LDG methods, the resulting implicit scheme is easy to implement and can be solved in an explicit way when it is coupled with iterative methods.

### 3.1. The nonlinear convection diffusion equation

We first consider a simple nonlinear convection diffusion equation in the domain  $\Omega = [0, 2\pi] \times [0, 2\pi]$  and with periodic boundary conditions

$$\omega_t + \omega \mathbf{V} \cdot \nabla \omega - \Delta \omega = 0, \tag{3.1}$$

where  $\mathbf{V} = [1, 1]^T$ . The convection term of equation (3.1) is in nonconservative form, which will lead to some instability for non-smooth exact solutions when the coefficient  $\mathbf{V}$  is very small. Thus, here we will study the convection diffusion equation with smooth exact solution.

To apply our proposed semi-implicit SDC method, it is necessary to construct a first order semi-implicit scheme firstly. Here, we treat both the convection and diffusion terms implicitly, and obtain a first order semi-implicit scheme as follows

$$\frac{\omega^{n+1} - \omega^n}{\Delta t} + \omega^n \mathbf{V} \cdot \nabla \omega^{n+1} - \Delta \omega^{n+1} = 0. \tag{3.2}$$

We test our numerical method taking the exact solution

$$\omega(x, y, t) = e^{-2t} \sin^2(x) \sin^2(y) \tag{3.3}$$

for equation (3.1) with a source term  $f(x, y, t)$ , which is a given function so that (3.3) is the exact solution.

The time step  $\Delta t$  is taken proportional to  $\Delta x$  such that  $\Delta t = 0.1\Delta x$ . Obviously, the condition would lead to some instabilities of the numerical solution for a fully explicit time marching method, since  $\Delta t = O(\Delta x^2)$  is necessary.

Table 3.1 presents the  $L^2$  and  $L^\infty$  errors and the numerical orders of accuracy at time  $T = 0.5$ , which shows  $(r + 1)$ -th order of accuracy in both  $L^2$  and  $L^\infty$  norms for  $\mathcal{P}^r$  approximation.

This example is designed to demonstrate that the our proposed semi-implicit SDC method is indeed efficient for nonlinear convection–diffusion equations, namely, we can get up to fourth order accuracy in both time and space with the time step proportional to  $\Delta x$ .

### 3.2. The surface diffusion and Willmore flow of flows

Xu and Shu [32] develop LDG methods for the surface diffusion of graphs

$$u_t + \nabla \cdot \left( Q \left( I - \frac{\nabla u \otimes \nabla u}{Q^2} \right) \nabla H \right) = 0, \tag{3.4}$$

and the Willmore flow of graphs

$$u_t + Q \nabla \cdot \left( \frac{1}{Q} \left( I - \frac{\nabla u \otimes \nabla u}{Q^2} \right) \nabla(QH) \right) - \frac{1}{2} Q \nabla \cdot \left( \frac{H^2}{Q} \nabla u \right) = 0, \tag{3.5}$$

where  $Q$  is the area element

**Table 3.2**  
Surface diffusion of graphs: accuracy test at time  $T = 0.5$ ,  $\Delta t = 0.1\Delta x$ .

|                 | $N$ | $L^2$ error | Order | $L^\infty$ error | Order |
|-----------------|-----|-------------|-------|------------------|-------|
| $\mathcal{P}^1$ | 16  | 1.50E-03    | –     | 1.34E-03         | –     |
|                 | 32  | 3.76E-04    | 1.99  | 3.38E-04         | 1.99  |
|                 | 64  | 9.43E-05    | 2.00  | 8.47E-05         | 2.00  |
| $\mathcal{P}^2$ | 16  | 1.07E-04    | –     | 1.22E-04         | –     |
|                 | 32  | 1.34E-05    | 3.00  | 1.53E-05         | 3.00  |
|                 | 64  | 1.68E-06    | 3.00  | 1.91E-06         | 3.00  |
| $\mathcal{P}^3$ | 16  | 5.43E-06    | –     | 7.01E-06         | –     |
|                 | 32  | 3.40E-07    | 4.00  | 4.40E-07         | 3.99  |
|                 | 64  | 2.14E-08    | 3.99  | 2.87E-08         | 3.94  |

$$Q = \sqrt{1 + |\nabla u|^2}$$

and  $H$  is mean curvature of the domain boundary  $\Gamma$

$$H = \nabla \cdot \left( \frac{\nabla u}{Q} \right),$$

which are high order accurate in space. According to the equations above, we can conclude that they are both highly nonlinear, and the stiff and non-stiff components can not be well separated, which increases the difficulty of developing semi-implicit time marching methods, not to mention high order schemes. Guo, Filbet and Xu develop a semi-implicit Runge–Kutta method to solve these two equations in [20]. However, only second order and third order accuracy are achieved. Motivated by the idea and the desire to develop a higher order scheme, we will apply the proposed semi-implicit SDC method here, which should be high order accurate and stable numerically.

To employ the semi-implicit SDC method, it is necessary to construct a first order semi-implicit scheme firstly. For the surface diffusion (3.4) and Willmore flow of graphs (3.5), we treat the linear part implicitly and the nonlinear part explicitly for simplicity and easy implementation. The corresponding first order semi-implicit schemes are

$$\begin{cases} \frac{u^{n+1} - u^n}{\Delta t} + \nabla \cdot \left( Q^n \left( I - \frac{\nabla u^n \otimes \nabla u^n}{(Q^n)^2} \right) \nabla \tilde{H}^{n+1} \right) = 0, \\ Q^n = \sqrt{1 + |\nabla u^n|^2}, \quad \tilde{H}^{n+1} = \nabla \cdot \left( \frac{\nabla u^{n+1}}{Q^n} \right), \end{cases} \tag{3.6}$$

for the surface diffusion of graphs (3.4) and

$$\begin{cases} \frac{u^{n+1} - u^n}{\Delta t} + Q^n \nabla \cdot \left( \frac{1}{Q^n} \left( I - \frac{\nabla u^n \otimes \nabla u^n}{(Q^n)^2} \right) \nabla (Q^n \tilde{H}^{n+1}) \right) - \frac{1}{2} Q^n \nabla \cdot \left( \frac{(H^n)^2}{Q^n} \nabla u^{n+1} \right) = 0, \\ Q^n = \sqrt{1 + |\nabla u^n|^2}, \quad \tilde{H}^{n+1} = \nabla \cdot \left( \frac{\nabla u^{n+1}}{Q^n} \right), \quad H^n = \nabla \cdot \left( \frac{\nabla u^n}{Q^n} \right), \end{cases} \tag{3.7}$$

for the Willmore flow of graphs (3.5). Then, we can employ the semi-implicit SDC method combining with the above first order schemes to obtain high order temporal accuracy. Next, we will present two numerical experiments to validate the result.

In both cases, the computational domains are  $\Omega = [-\pi, \pi] \times [-\pi, \pi]$ , with periodic boundary conditions. For the surface diffusion of graphs (3.4), we consider the accuracy test taking the exact solution

$$u(x, y, t) = 0.05e^{-2t} \sin(x + y) \tag{3.8}$$

for equation (3.4) with a source term  $f(x, y, t)$ , which is a given function so that (3.8) is the exact solution. The time step is taken as  $\Delta t = 0.1\Delta x$ . The  $L^2$  and  $L^\infty$  errors and the numerical orders of accuracy at time  $T = 0.5$  are obtained in Table 3.2, which shows  $(r + 1)$ -th order of accuracy in both  $L^2$  and  $L^\infty$  norms for  $\mathcal{P}^r$  approximation, i.e. our numerical scheme is more accurate for larger time steps comparing with other existing numerical methods.

We present in Fig. 3.1 the time evolution of the  $L^2$  norm of the numerical solution, and the functional  $\mathcal{E}_{SD}(t)$  is defined by

$$\mathcal{E}_{SD}(t) = \frac{1}{2} \int_{\Omega} u^2(t, \mathbf{x}) d\mathbf{x}.$$

The result shows that our semi-implicit SDC time marching method is stable numerically with large time steps.

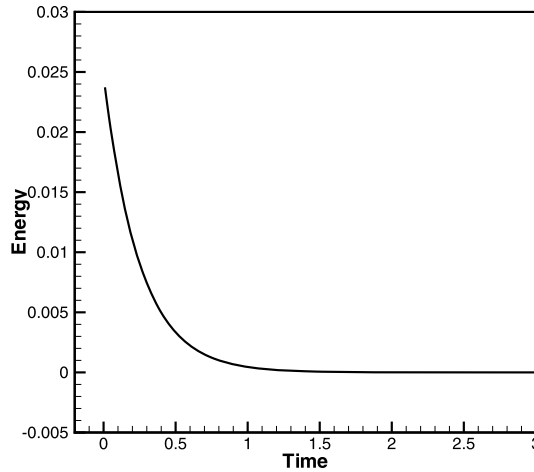


Fig. 3.1. Surface diffusion of graphs: time evolution of  $L^2$  norm obtained with LDG spatial discretization and the semi-implicit SDC time marching method.

Table 3.3

Willmore flow of graphs: accuracy test at time  $T = 0.5$ ,  $\Delta t = 0.1\Delta x$ .

|                 | $N$ | $L^2$ error | Order | $L^\infty$ error | Order |
|-----------------|-----|-------------|-------|------------------|-------|
| $\mathcal{P}^1$ | 16  | 1.50E-03    | –     | 1.34E-03         | –     |
|                 | 32  | 3.76E-04    | 1.99  | 3.38E-04         | 1.99  |
|                 | 64  | 9.43E-05    | 2.00  | 8.47E-05         | 2.00  |
| $\mathcal{P}^2$ | 16  | 1.07E-04    | –     | 1.22E-04         | –     |
|                 | 32  | 1.34E-05    | 3.00  | 1.53E-05         | 3.00  |
|                 | 64  | 1.68E-06    | 3.00  | 1.91E-06         | 3.00  |
| $\mathcal{P}^3$ | 16  | 5.43E-06    | –     | 7.01E-06         | –     |
|                 | 32  | 3.40E-07    | 4.00  | 4.40E-07         | 3.99  |
|                 | 64  | 2.14E-08    | 3.99  | 2.87E-08         | 3.94  |

For the Willmore flow of graphs (3.5), we test our scheme taking the exact solution

$$u(x, y, t) = 0.05e^{-2t} \sin(x + y) \tag{3.9}$$

for equation (3.5) with a source term  $f(x, y, t)$ , which is a given function so that (3.9) is the exact solution. The time step is taken as  $\Delta t = 0.1\Delta x$ . The  $L^2$  and  $L^\infty$  errors and the numerical orders of accuracy at time  $T = 0.5$  are obtained in Table 3.3, which also shows  $(r + 1)$ -th order of accuracy in both  $L^2$  and  $L^\infty$  norms for  $\mathcal{P}^r$  approximation.

We present in Fig. 3.2 the time evolution of the energy of the numerical solution, and the functional  $\mathcal{E}_W(t)$  is defined by

$$\mathcal{E}_W(t) = \frac{1}{2} \int_{\Omega} H^2(t, \mathbf{x}) Q(t, \mathbf{x}) d\mathbf{x}.$$

From Fig. 3.2, we can see that our numerical scheme is energy stable numerically, namely, the discrete energy is always non-increasing with respect to time.

The higher order differential operators and additional nonlinearities for the surface diffusion and Willmore flows of graphs are difficult to simulate numerically, especially for high order spatial and time discretization methods. Numerical results show that the proposed semi-implicit SDC method is indeed efficient for highly nonlinear PDEs containing high order spatial derivatives (see Tables 3.2–3.3).

### 3.3. The Cahn–Hilliard equation

In this subsection, we consider the Cahn–Hilliard equation

$$u_t = \nabla \cdot (b(u)\nabla(-\gamma \Delta u + u^3 - u)), \tag{3.10}$$

where  $b(u)$  is the degenerate mobility, and  $\gamma$  is a positive constant. The Cahn–Hilliard equation (3.10) is a gradient flow in the Hilbert space  $H^{-1}$  with the energy functional

$$E(u) = \int_{\Omega} \left( \frac{1}{2} \gamma |\nabla u|^2 + F(u) \right) d\mathbf{x}. \tag{3.11}$$

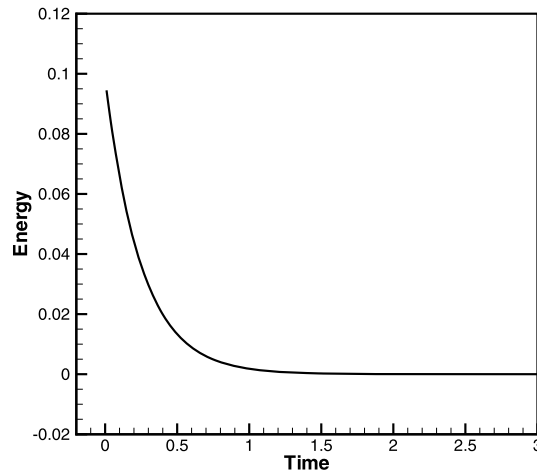


Fig. 3.2. Willmore flow of graphs: energy curves obtained with LDG spatial discretization and the semi-implicit SDC time marching method.

Table 3.4

Cahn–Hilliard equation: accuracy test at time  $T = 0.5$ ,  $\Delta t = 0.1\Delta x$ .

|                 | $N$ | $L^2$ error | Order | $L^\infty$ error | Order |
|-----------------|-----|-------------|-------|------------------|-------|
| $\mathcal{P}^1$ | 16  | 2.12E-02    | –     | 1.54E-02         | –     |
|                 | 32  | 5.33E-03    | 2.00  | 3.89E-03         | 1.99  |
|                 | 64  | 1.33E-03    | 2.00  | 9.72E-04         | 2.00  |
| $\mathcal{P}^2$ | 16  | 1.38E-03    | –     | 1.23E-03         | –     |
|                 | 32  | 1.70E-04    | 3.02  | 1.55E-04         | 2.99  |
|                 | 64  | 2.13E-05    | 3.00  | 1.96E-05         | 2.98  |
| $\mathcal{P}^3$ | 16  | 6.80E-05    | –     | 8.66E-05         | –     |
|                 | 32  | 4.25E-06    | 4.00  | 5.51E-06         | 3.97  |
|                 | 64  | 2.66E-07    | 4.00  | 3.47E-07         | 3.99  |

Various numerical simulations have been developed for the Cahn–Hilliard equation [14,15,17,24] recently. For example, Feng et al. [15] developed a high order and energy stable scheme to simulate phase field models with constant mobility by combining the classical semi-implicit SDC method and energy stable convex splitting technique. However, these methods are mainly efficient for phase field problems with constant mobility.

The Cahn–Hilliard equation (3.10) with degenerate mobility is highly nonlinear, which increases the difficulty of designing high order time marching methods. Because in this case, the stiff and non-stiff components can not be well separated, which leads to that the use of traditional implicit-explicit methods is not straightforward. In this paper, we will apply our semi-implicit SDC method to solve the Cahn–Hilliard equation with degenerate mobility, obtaining high order temporal accuracy.

In order to apply the SDC method, we shall first present a first order semi-implicit method. The first order convex splitting scheme proposed in [17] is given in the following form

$$\frac{u^{n+1} - u^n}{\Delta t} = \nabla \cdot \left[ b(u^n) \nabla \left( -\gamma \Delta u^{n+1} + (u^{n+1})^3 - u^n \right) \right], \quad (3.12)$$

which is unconditionally energy stable. Then we can therefore employ the semi-implicit SDC method combining with the convex splitting scheme (3.12). Next, we will perform an accuracy test to show our result.

We consider the Cahn–Hilliard equation (3.10) with  $b(u) = 1 - u^2$ ,  $\gamma = 1.0$  in the square domain  $\Omega = [0, 2\pi] \times [0, 2\pi]$  and with periodic boundary condition. For the tests, we take the exact solution of

$$u(x, y, t) = e^{-2t} \sin(x) \sin(y), \quad (3.13)$$

with a source term  $f(x, y, t)$ , where  $f(x, y, t)$  is a given function so that (3.13) is the exact solution.

Table 3.4 presents the accuracy and order in  $L^2$  and  $L^\infty$  norms, which gives the expected optimal convergence rate. The time step  $\Delta t$  is taken proportional to  $\Delta x$  such that  $\Delta t = \lambda \Delta x$ , with  $\lambda = 0.1$ .

The energy trace is presented in Fig. 3.3, we can see that the discrete energy is non-increasing in time, which shows that our semi-implicit SDC method combining with the unconditionally stable convex splitting scheme (3.12) can maintain the energy stability numerically when solving the Cahn–Hilliard equation.

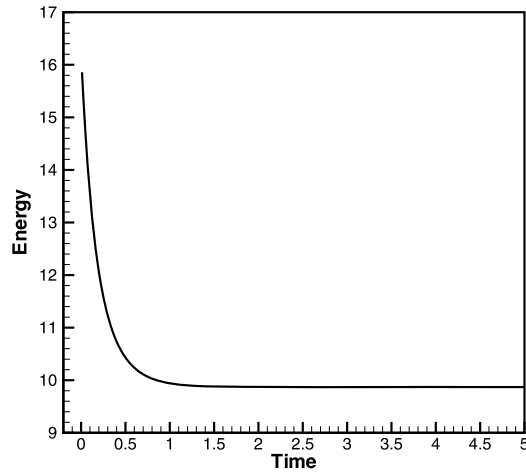


Fig. 3.3. Cahn–Hilliard equation: energy curves obtained with LDG spatial discretization and the semi-implicit SDC time marching method.

### 3.4. The Cahn–Hilliard–Brinkman system

In this subsection, we consider the Cahn–Hilliard–Brinkman (CHB) system

$$\begin{cases} \phi_t = \nabla \cdot (M(\phi)\nabla\mu) - \nabla \cdot (\phi\mathbf{u}), \\ \mu = \phi^3 - \phi - \varepsilon^2\Delta\phi, \\ -\nabla \cdot [v(\phi)\mathbf{D}(\mathbf{u})] + \eta(\phi)\mathbf{u} = -\nabla p - \gamma\phi\nabla\mu, \\ \nabla \cdot \mathbf{u} = 0, \end{cases} \quad (3.14)$$

where  $M(\phi) > 0$  is a mobility that incorporates the Peclet number,  $\mathbf{u}$  is the advective velocity,  $p$  is the pressure and  $\mathbf{D}(\mathbf{u}) = \nabla\mathbf{u} + (\nabla\mathbf{u})^T$ .

The CHB system is energy dissipative, *i.e.*

$$\frac{d}{dt}E = - \int_{\Omega} \left( M(\phi)|\nabla\mu|^2 + \frac{1}{\gamma}\eta(\phi)|\mathbf{u}|^2 + \frac{1}{2\gamma}v(\phi)|\mathbf{D}(\mathbf{u})|^2 \right) d\mathbf{x} \leq 0, \quad (3.15)$$

where the Ginzburg–Landau free energy  $E$  is given by

$$E(\phi) = \int_{\Omega} \left\{ \frac{\varepsilon^2}{2}|\nabla\phi|^2 + \frac{1}{4}(\phi^2 - 1)^2 \right\} d\mathbf{x}. \quad (3.16)$$

A few numerical simulations have been developed to solve the CHB system. For example, Collins et al. [12] presented a first order unconditionally energy stable and uniquely solvable finite difference scheme for the CHB system. Guo and Xu [18] developed efficient unconditionally energy stable convex splitting LDG scheme for the CHB system. To our knowledge, the existing temporal methods for solving the CHB system are all first order accurate, such as the convex splitting scheme proposed in [18]

$$\begin{cases} \frac{\phi^{n+1} - \phi^n}{\Delta t} = \nabla \cdot (M(\phi^n)\nabla\mu^{n+1}) - \nabla \cdot (\phi^n\mathbf{u}^{n+1}), \\ \mu^{n+1} = (\phi^{n+1})^3 - \phi^n - \varepsilon^2\Delta\phi^{n+1}, \\ -\nabla \cdot [v(\phi^n)\mathbf{D}(\mathbf{u}^{n+1})] + \eta(\phi^n)\mathbf{u}^{n+1} = -\nabla p^{n+1} - \gamma\phi^n\nabla\mu^{n+1}, \\ \nabla \cdot \mathbf{u}^{n+1} = 0. \end{cases} \quad (3.17)$$

The CHB system is a highly nonlinear phase field model, and obviously the stiff and non-stiff components of the system can not be well separated. Therefore, the first order convex splitting scheme (3.17) is not easy to extend to higher order accurate ones. And the design of high order time marching methods will be incredibly difficult. In this case, based on the convex splitting scheme (3.17), we will apply the proposed semi-implicit SDC method to achieve high order temporal accuracy. Next, we will first validate the result via an accuracy test, and then present a long time simulation to investigate the long time behavior of the numerical solution obtained from the proposed SDC method.

**Table 3.5**  
Cahn–Hilliard–Brinkman system: accuracy test at time  $T = 0.4$ ,  $\Delta t = 0.1\Delta x$ .

|                 | $N$ | $L^2$ error | Order | $L^\infty$ error | Order |
|-----------------|-----|-------------|-------|------------------|-------|
| $\mathcal{P}^1$ | 16  | 2.59E–02    | –     | 1.88E–02         | –     |
|                 | 32  | 6.51E–03    | 1.99  | 4.74E–03         | 1.99  |
|                 | 64  | 1.62E–03    | 2.00  | 1.18E–03         | 2.00  |
| $\mathcal{P}^2$ | 16  | 1.74E–03    | –     | 1.63E–03         | –     |
|                 | 32  | 2.26E–04    | 2.94  | 2.06E–04         | 2.98  |
|                 | 64  | 2.87E–05    | 2.97  | 2.59E–05         | 2.99  |
| $\mathcal{P}^3$ | 16  | 8.36E–05    | –     | 1.08E–04         | –     |
|                 | 32  | 5.41E–06    | 3.95  | 7.19E–06         | 3.91  |
|                 | 64  | 3.76E–07    | 3.85  | 5.07E–07         | 3.83  |

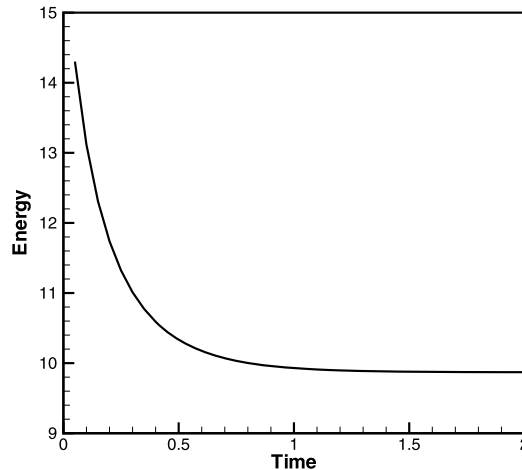


**Fig. 3.4.** Cahn–Hilliard–Brinkman system: energy curves obtained with LDG spatial discretization and the semi-implicit SDC time marching method.

*Accuracy test*

We consider the CHB system (3.14) with  $M(\phi) = 1$ ,  $\eta(\phi) = 1$ ,  $\nu(\phi) = 1$ ,  $\varepsilon = 1$ ,  $\gamma = 1$  in the square domain  $\Omega = [0, 2\pi] \times [0, 2\pi]$  and with periodic boundary condition. For the tests, we take the exact solution of

$$\phi(x, y, t) = e^{-2t} \sin(x) \sin(y), \tag{3.18}$$

with a source term  $f(x, y, t)$ , where  $f(x, y, t)$  is a given function so that (3.18) is the exact solution. Table 3.5 presents the accuracy and order in  $L^2$  and  $L^\infty$  norms, which shows up to fourth order accuracy in both time and space.

The energy trace is presented in Fig. 3.4, we can see that the discrete energy is non-increasing in time, which shows that our semi-implicit SDC method is stable numerically.

*Buoyancy-driven flows of the CHB system*

To simulate buoyancy-driven flow, we replace the Brinkman flow by

$$-\nabla \cdot [\nu(\phi)D(\mathbf{u})] + \eta(\phi)\mathbf{u} + \nabla p = -\gamma\phi\nabla\mu + \mathbf{b}, \tag{3.19}$$

where  $\mathbf{b}$  is a buoyancy term that depends on the mass density. The mass density is assumed depend on  $\phi$ , i.e.  $\rho = \rho(\phi)$ , and we employ a Boussinesq type approximation:

$$\mathbf{b} = -b(\phi)\widehat{\mathbf{k}}, \quad b(\phi) = \chi(\phi - \phi_0), \tag{3.20}$$

where  $\phi_0$  is a constant (usually the average value of  $\phi$ ), and  $\chi$  is a constant. Thus, the corresponding convex-splitting scheme that we use for the buoyancy-driven flow is

$$-\nabla \cdot [\nu(\phi^n)D(\mathbf{u}^{n+1})] + \eta(\phi^n)\mathbf{u}^{n+1} = -\nabla p^{n+1} - \gamma\phi^n\nabla\mu^{n+1} - b(\phi^n)\widehat{\mathbf{k}}. \tag{3.21}$$

The physical parameters are  $\varepsilon = 0.03$ ,  $\gamma = 4.0\varepsilon$ ,  $\phi_0 = \bar{\phi} = -0.05$ ,  $\chi = 10$ ,  $\eta = 1$  and  $\nu = 1$ . We take the mobility to be

$$M(\phi) = \sqrt{(1 + \phi)^4(1 - \phi)^4 + \varepsilon^2}. \tag{3.22}$$

The initial data is a random field of values that are uniformly distributed about the average composition  $\bar{\phi} = -0.05$ , with amplitude 0.05. The domain is  $[0, 6.4] \times [0, 6.4]$ . The boundary conditions are

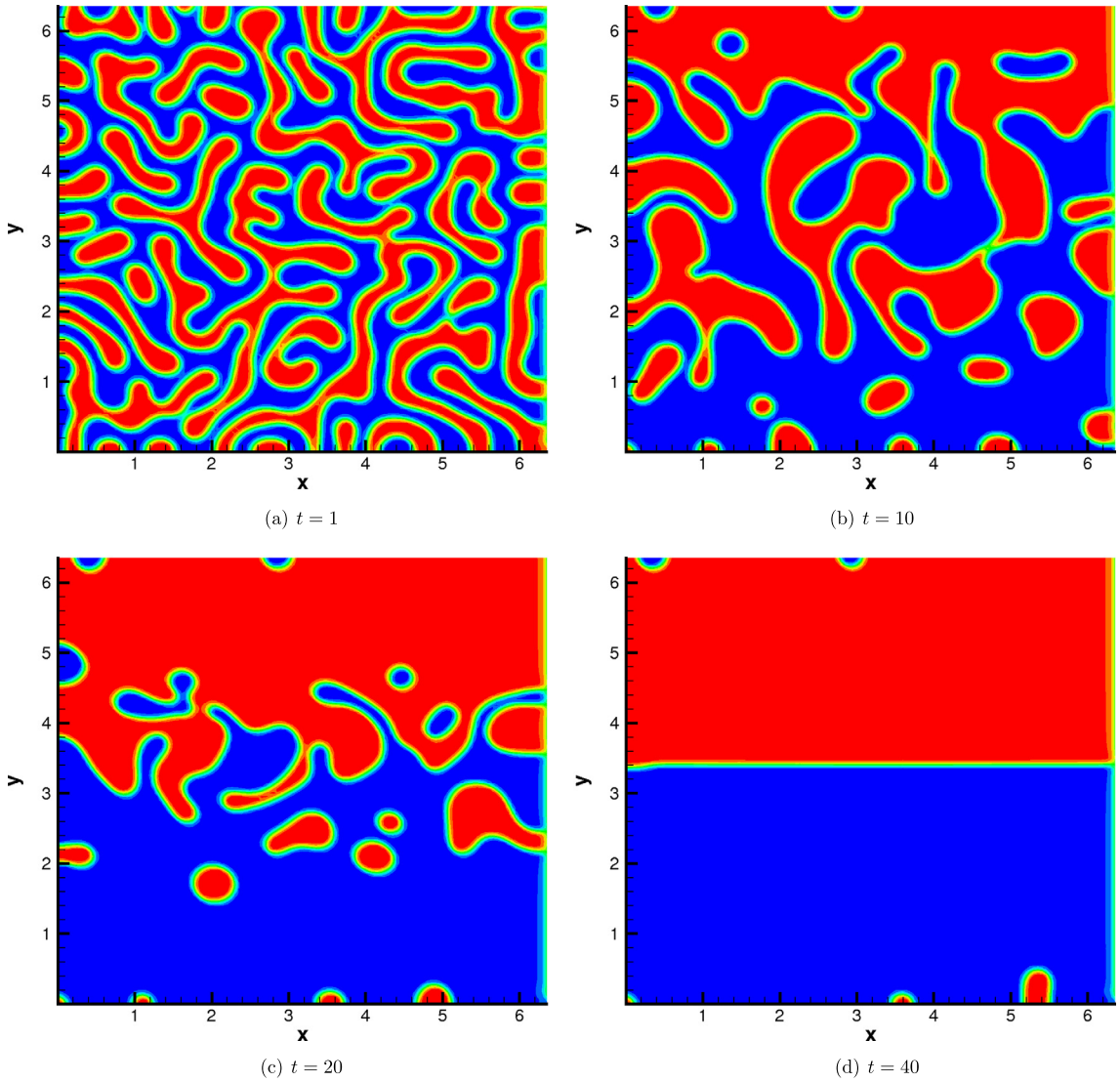


Fig. 3.5. Numerical solutions of the CHB system obtained using the third order semi-implicit SDC method.

$$\mathbf{u} = 0, \quad \partial_n \phi = \partial_n \mu = 0 \quad \text{on} \quad \partial\Omega. \tag{3.23}$$

We use a  $128 \times 128$  uniform mesh and the piecewise  $\mathcal{P}^2$  approximation. Fig. 3.5 presents numerical solutions using the third order semi-implicit SDC method with  $\Delta t = 0.01$ . It is observed that the solution dynamics can be captured quite well. The energy evolution is presented in Fig. 3.6, which is non-increasing in time.

Phase field models have been widely used and attracted much attention, especially for the exploration of efficient semi-implicit time marching methods. The existing temporal methods are mainly first or second order convex splitting schemes. Specially, the semi-implicit SDC method proposed in this paper is a novel high order scheme when solving the CHB system. The strategy presented in this paper can be easily generalized to other phase field problems, e.g. the Cahn–Hilliard–Hele–Shaw system.

### 3.5. The phase field crystal equation

In this subsection, we consider the sixth order nonlinear phase field crystal (PFC) equation

$$\begin{cases} \phi_t = \nabla \cdot (M(\phi)\nabla\mu), \\ \mu = \phi^3 + (1 - \epsilon)\phi + 2\Delta\phi + \Delta^2\phi, \end{cases} \tag{3.24}$$

where  $M(\phi) \geq 0$  is a mobility. The gradient flow (3.24) is mass preserving and the total energy decays with respect to time  $t$ , namely,  $\frac{d}{dt}E \leq 0$ , where the energy functional  $E$  is of the form

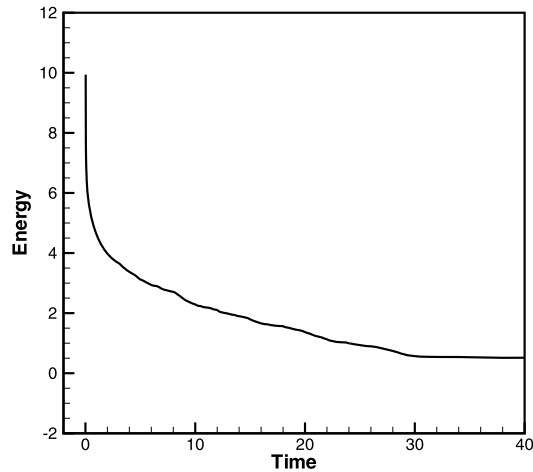


Fig. 3.6. The discrete energy traces of the CHB system.

$$E(\phi) = \int_{\Omega} \left\{ \frac{1}{4} \phi^4 + \frac{1-\epsilon}{2} \phi^2 - |\nabla \phi|^2 + \frac{1}{2} (\Delta \phi)^2 \right\} d\mathbf{x}. \quad (3.25)$$

Various unconditionally stable first order and second order temporal discretization schemes coupled with finite difference methods [23,28], finite element methods [16] and local discontinuous Galerkin method [19] have been developed for the PFC equation recently. Unfortunately, the proposed convex splitting schemes are only first order or second order accurate in time. Guo and Xu [19] applied the semi-implicit SDC method to achieve high order temporal accuracy, but it was only efficient for the PFC equation with constant mobility.

Here, we will develop a new semi-implicit SDC method to solve the PFC equation with degenerate mobility. Firstly, it is necessary to develop a first order convex splitting scheme

$$\begin{cases} \frac{\phi^{n+1} - \phi^n}{\Delta t} = \nabla \cdot (M(\phi^n) \nabla \mu^{n+1}), \\ \mu^{n+1} = (\phi^{n+1})^3 + (1-\epsilon)\phi^{n+1} + 2\Delta\phi^n + \Delta^2\phi^{n+1}. \end{cases} \quad (3.26)$$

We have proved the unconditional energy stability of the convex splitting scheme (3.26) coupled with LDG spatial discretization in [19]. Then the proposed semi-implicit SDC method can be driven iteratively by the chosen low order method (3.26). Next, we will present a numerical experiment to validate the result.

We consider the accuracy test for the PFC equation (3.24) with degenerate mobility, i.e.  $M(\phi) = 1 - \phi^2$  on the domain  $[0, 2\pi] \times [0, 2\pi]$  with periodic boundary conditions. For the tests we take the exact solution of

$$\phi(x, y, t) = e^{-2t} \sin(x) \sin(y), \quad (3.27)$$

with the source term  $f(x, y, t)$ , where  $f(x, y, t)$  is a given function so that (3.27) is the exact solution of the PFC equation. Choose the parameter  $\epsilon = 0.5$ . Table 3.6 presents the  $L^2$  and  $L^\infty$  errors and numerical orders of accuracy at time  $T = 0.5$ , which shows that the semi-implicit SDC method coupled with  $\mathcal{P}^r$  approximation gives a  $(r+1)$ -th order of accuracy for the PFC equation with degenerate mobility.

The energy trace is presented in Fig. 3.7, we can see that the discrete energy is non-increasing in time, which shows that our semi-implicit SDC method combining with the unconditionally stable convex splitting scheme (3.26) can maintain the stability numerically when solving the PFC equation with degenerate mobility.

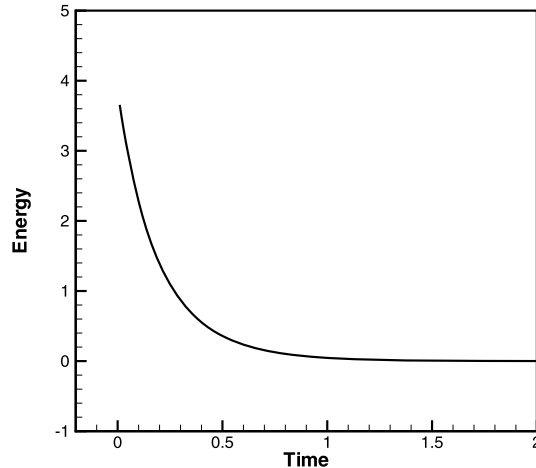
Although we developed high order time marching methods for the PFC equation in [19], the classical SDC method is not efficient for the PFC equation with degenerate mobility. The semi-implicit Runge–Kutta successfully overcome this difficulty, however, we only obtain up to third order temporal accuracy. From the above example, it is easy to construct higher order scheme and we can achieve a fourth order accuracy with our new semi-implicit SDC method.

#### 4. Concluding remarks

We presented in this paper a novel semi-implicit spectral deferred correction (SDC) time marching method, which are motivated by the desire to design higher order temporal methods for PDEs without easily separating of stiff and non-stiff components. Combined with the local discontinuous Galerkin method, this SDC method has been applied on a series of highly nonlinear PDEs, including the nonlinear convection diffusion equation, the surface diffusion and Willmore flow of graphs, the Cahn–Hilliard equation with degenerate mobility, the Cahn–Hilliard–Brinkman system and the phase field

**Table 3.6**Phase field crystal equation: accuracy test at time  $T = 0.5$ ,  $\Delta t = 0.1 \Delta x$ .

|                 | $N$ | $L^2$ error | Order | $L^\infty$ error | Order |
|-----------------|-----|-------------|-------|------------------|-------|
| $\mathcal{P}^1$ | 16  | 2.12E-02    | –     | 1.50E-02         | –     |
|                 | 32  | 5.33E-03    | 2.00  | 3.81E-03         | 1.98  |
|                 | 64  | 1.33E-03    | 2.00  | 9.57E-04         | 1.99  |
| $\mathcal{P}^2$ | 16  | 1.40E-03    | –     | 1.25E-03         | –     |
|                 | 32  | 1.71E-04    | 3.03  | 1.55E-04         | 3.00  |
|                 | 64  | 2.12E-05    | 3.01  | 1.93E-05         | 3.00  |
| $\mathcal{P}^2$ | 16  | 1.08E-05    | –     | 8.64E-05         | –     |
|                 | 32  | 6.78E-07    | 4.00  | 5.46E-06         | 3.98  |
|                 | 64  | 4.29E-08    | 3.98  | 3.37E-07         | 4.01  |

**Fig. 3.7.** Phase field crystal equation: energy curves obtained with LDG spatial discretization and the semi-implicit SDC time marching method.

crystal equation. These fully discrete schemes can achieve arbitrary high order accuracy and stability with the time step proportional to the spatial mesh size. We conclude that the proposed semi-implicit SDC method is effective and robust when solving highly nonlinear PDEs, preserving high order accuracy and good stability. In addition, it is believable that the new semi-implicit SDC method can be applied to solve many other PDEs beyond those presented in this paper.

## References

- [1] U.M. Ascher, L.R. Petzold, *Computer Methods for Ordinary Differential Equations and Differential-Algebraic Equations*, SIAM, Philadelphia, PA, 2000.
- [2] S. Boscarino, F. Filbet, G. Russo, High order semi-implicit schemes for time dependent partial differential equations, *J. Sci. Comput.* 68 (2016) 975–1001.
- [3] A. Brandt, *Multigrid Techniques: 1984 Guide with Applications to Fluid Dynamics*, GMD-Studien (GMD Studies), vol. 85, Gesellschaft für Mathematik und Datenverarbeitung mbH, St. Augustin, 1984.
- [4] J.C. Butcher, *The Numerical Analysis of Ordinary Differential Equations: Runge–Kutta and General Linear Methods*, John Wiley and Sons, Chichester, 1987.
- [5] B. Cockburn, C.-W. Shu, TVB Runge–Kutta local projection discontinuous Galerkin finite element method for conservation laws II: general framework, *Math. Comput.* 52 (1989) 411–435.
- [6] B. Cockburn, S.-Y. Lin, C.-W. Shu, TVB Runge–Kutta local projection discontinuous Galerkin finite element method for conservation laws III: one dimensional systems, *J. Comput. Phys.* 84 (1989) 90–113.
- [7] B. Cockburn, S. Hou, C.-W. Shu, The Runge–Kutta local projection discontinuous Galerkin finite element method for conservation laws IV: the multidimensional case, *Math. Comput.* 54 (1990) 545–581.
- [8] B. Cockburn, C.-W. Shu, The Runge–Kutta discontinuous Galerkin method for conservation laws V: multidimensional systems, *J. Comput. Phys.* 141 (1998) 199–224.
- [9] B. Cockburn, C.-W. Shu, The local discontinuous Galerkin method for time-dependent convection–diffusion systems, *SIAM J. Numer. Anal.* 35 (1998) 2440–2463.
- [10] B. Cockburn, Discontinuous Galerkin methods for convection-dominated problems, in: T.J. Barth, H. Deconinck (Eds.), *High-Order Methods for Computational Physics*, in: *Lecture Notes in Computational Science and Engineering*, vol. 9, Springer, 1999, pp. 69–224.
- [11] B. Cockburn, C.-W. Shu, The local discontinuous Galerkin method for time-dependent convection–diffusion systems, *SIAM J. Numer. Anal.* 35 (1998) 2440–2463.
- [12] C. Collins, J. Shen, S.M. Wise, An efficient, energy stable scheme for the Cahn–Hilliard–Brinkman system, *Commun. Comput. Phys.* 13 (2013) 929–957.
- [13] A. Dutt, L. Greengard, V. Rikhlin, Spectral deferred correction methods for ordinary differential equations, *BIT Numer. Math.* 40 (2000) 241–266.
- [14] D.J. Eyre, Unconditionally gradient stable time marching the Cahn–Hilliard equation, in: J.W. Bullard, R. Kalia, M. Stoneham, L.Q. Chen (Eds.), *Computational and Mathematical Models of Microstructural Evolution*, vol. 53, Materials Research Society, Warrendale, 1998, pp. 1686–1712.
- [15] X. Feng, T. Tang, J. Yang, Long time numerical simulations for phase-field problems using  $p$ -adaptive spectral deferred correction methods, *SIAM J. Sci. Comput.* 37 (2015) A271–A294.

- [16] H. Gomez, X. Nogueira, An unconditionally energy-stable method for the phase field crystal equation, *Comput. Methods Appl. Mech. Eng.* 249 (2012) 52–61.
- [17] R. Guo, Y. Xu, Efficient solvers of discontinuous Galerkin discretization for the Cahn–Hilliard equation, *J. Sci. Comput.* 58 (2014) 380–408.
- [18] R. Guo, Y. Xu, An efficient, unconditionally energy stable local discontinuous Galerkin scheme for the Cahn–Hilliard–Brinkman system, *J. Comput. Phys.* 298 (2015) 387–405.
- [19] R. Guo, Y. Xu, Local discontinuous Galerkin method and high order semi-implicit scheme for the phase field crystal equation, *SIAM J. Sci. Comput.* 38 (2016) A105–A127.
- [20] R. Guo, F. Filbet, Y. Xu, Efficient high order semi-implicit time discretization and local discontinuous Galerkin methods for highly nonlinear PDEs, *J. Sci. Comput.* 68 (2016) 1029–1054.
- [21] E. Hairer, S.P. Norsett, G. Wanner, *Solving Ordinary Differential Equations I, Nonstiff Problems*, Springer-Verlag, Berlin, 1987.
- [22] E. Hairer, G. Wanner, *Solving Ordinary Differential Equations II, Stiff and Differential-Algebraic Problems*, Springer-Verlag, Berlin, 1991.
- [23] Z. Hu, S.M. Wise, C. Wang, J.S. Lowengrub, Stable and efficient finite-difference nonlinear-multigrid schemes for the phase field crystal equation, *J. Comput. Phys.* 228 (2009) 5323–5339.
- [24] F. Liu, J. Shen, Stabilized semi-implicit spectral deferred correction methods for Allen–Cahn and Cahn–Hilliard equations, *Math. Methods Appl. Sci.* 38 (2015) 4564–4575.
- [25] M. Minion, Semi-implicit spectral deferred correction methods for ordinary differential equations, *Commun. Math. Sci.* 1 (2003) 471–500.
- [26] W.H. Reed, T.R. Hill, *Triangular Mesh Method for the Neutron Transport Equation*, Technical report LA-UR-73-479, Los Alamos Scientific Laboratory, Los Alamos, NM, 1973.
- [27] T. Tang, H. Xie, X. Yin, High-order convergence of spectral deferred correction methods on general quadrature nodes, *J. Sci. Comput.* 56 (2012) 1–13.
- [28] S.M. Wise, C. Wang, J.S. Lowengrub, An energy-stable and convergent finite-difference scheme for the phase field crystal equation, *SIAM J. Numer. Anal.* 44 (2009) 2269–2288.
- [29] Y. Xia, Y. Xu, C.-W. Shu, Efficient time discretization for local discontinuous Galerkin methods, *Discrete Contin. Dyn. Syst., Ser. B* 8 (2007) 677–693.
- [30] Y. Xia, Y. Xu, C.-W. Shu, Local discontinuous Galerkin methods for the Cahn–Hilliard type equations, *J. Comput. Phys.* 227 (2007) 472–491.
- [31] Y. Xia, A fully discrete stable discontinuous Galerkin method for the thin film epitaxy problem without slope selection, *J. Comput. Phys.* 280 (2015) 248–260.
- [32] Y. Xu, C.-W. Shu, Local discontinuous Galerkin method for surface diffusion and Willmore flow of graphs, *J. Sci. Comput.* 40 (2009) 375–390.
- [33] Y. Xu, C.-W. Shu, Local discontinuous Galerkin methods for high-order time-dependent partial differential equations, *Commun. Comput. Phys.* 7 (2010) 1–46.